Acta Cryst. (1979). B35, 2580–2593

Single-Crystal Structures and Electron Density Distributions of Ethane, Ethylene and Acetylene.
II.* Single-Crystal X-ray Structure Determination of Acetylene at 141 K

BY GERARD J. H. VAN NES AND FRÉ VAN BOLHUIS

Laboratorium voor Structuurchemie, Rijksuniversiteit Groningen, Nijenborgh 16, 9747 *AG, Groningen, The Netherlands*

(*Received* 27 *November* 1978; *accepted* 11 *June* 1979)

Abstract

Crystalline acetylene at 141 K is cubic, $a = 6{\cdot}091$ (3) Å, space group $Pa3$, $Z = 4$. The intensities of all 164 independent reflexions up to $\sin\theta/\lambda = 0{\cdot}80$ Å^{-1} were measured accurately on a Nonius four-circle diffractometer. For higher $\sin\theta/\lambda$, very few significant reflexion intensities exist due to the strong thermal motion. A valence analysis, with multipole deformation terms and restricted radial functions centred on the atoms, was performed for the 164 independent reflexions by least-squares refinement on I. Both ζ and SCF scattering factors were considered. H was constrained to C. The radial functions corresponding to the SCF scattering factors were modified by introduction of an isotropic extinction parameter and an additional isotropic temperature factor for H in the refinement. $R_w(I;\zeta) = 0{\cdot}0176$ and $R_w(I;\mathrm{SCF}) = 0{\cdot}0170$, both with 11 independent parameters. Third and fourth cumulant terms describing the non-linearity of the librational motion had no significant effect. Filtered and unfiltered maps including multipole deformations only are based on the 138 reflexions with $I \geq 0$. For the (modified) SCF atomic scattering factors the agreement with theory is better than for the ζ scattering factors. In the present analysis static deformations and thermal smearing could not be separated and no reliable value could be found for the scale factor. The situation would be more favourable for compounds with smaller thermal motion for which both X-ray and neutron data are available.

1. Introduction

In our attempts to obtain accurate crystal structures and electron density distributions of ethane, ethylene and acetylene by X-ray diffraction, acetylene was the first compound to be studied (van Nes & van Bolhuis, 1975). In the last few years several improvements were made both in the technique for growing single crystals of volatile (small molecule) compounds and in the cooling equipment for obtaining stable low temperatures (van Nes & van Bolhuis, 1978). In spite of this, slow progress has been made with the acetylene work as it has not yet been possible to collect accurate intensities for the orthorhombic phase (stable below 133 K). After many attempts, a single-crystal X-ray data set at 141 K was obtained which was considered as optimal for the high-temperature cubic phase. The present paper reports the structure refinement and the difficulties encountered by limitations of the data set, especially due to lack of reliable reflexion intensities above $\sin\theta/\lambda = 0{\cdot}80$ Å^{-1}, caused by the high thermal motion of the molecules.

2. Earlier crystallographic and spectral work

As early as 1913 optical studies by Wahl (1913) revealed the existence of an optical isotropic phase and a strongly doubly refracting anisotropic phase for acetylene. Unsuccessful attempts to determine the structures by X-ray diffraction were made by Mooy (1932) and by Washer (1935). Sugawara & Kanda (1952) determined the approximate structure of the cubic phase at 156 K from visually estimated X-ray intensities of a single crystal (Table 1). Their reported (first-order) transition to an orthorhombic modification at 133 K is consistent with many later spectroscopic experiments (Krikorian, 1957; Bottger & Eggers, 1964, 1966; Anderson & Smith, 1966; Smith, 1969; Ito, Yokoyama & Suzuki, 1970). A few years ago, the structure of this orthorhombic modification was determined by neutron diffraction at 4·2 K (Koski, 1975*a*; Koski & Sándor, 1975), at 77 K (Koski, 1975*b*), and at 109 K (Koski, 1975*c*). Moreover an anisotropic refinement based on powder neutron diffraction data (Koski, 1975*d*) was carried out for the cubic modification of C_2D_2 which, however, did not result in a very accurate structure (Table 1). It should be noted that the thermal parameters found by Koski

* Part I: van Nes & Vos (1978).

0567-7408/79/112580-14$01.00

Table 1. *Structural data for acetylene*

	C_2H_2	C_2D_2	C_2H_2	C_2D_2
Reference*	I (1952)	II (1975)	This paper	III (1975)
Technique	X-ray single crystal	Neutron powder	X-ray single crystal	Neutron powder
Temperature (K)	156	150·5	141	4·2
Space group	*Pa*3	*Pa*3	*Pa*3	*Acam*
Z	4	4	4	4
a,b,c (Å)	6·14 (1)	6·12 (1)	6·091 (3)†	6·193 (3), 6·005 (3) 5·551 (3)
Site symmetry of molecule	$\bar{3}$	$\bar{3}$	$\bar{3}$	*m*
Number of reflexions	47	15	164	28
$(\sin\theta/\lambda)_{max}$ (Å^{-1})	0·53	0·41	0·80	0·43
$R_w(I)$	–	0·14‡	0·0170§	0·0367‡
C≡C (Å)	1·20 (2)	1·15 (1)	1·178 (2)§	1·180 (6)
C–H (Å)	1·05 (5)	1·06 (1)	1·043 (–)§	1·061 (5)

* (I) Sugawara & Kanda (1952); (II) Koski (1975*d*); (III) Koski (1975*a*), Koski & Sándor (1975).
† a(134 K) = 6·081 (3) Å, a (176 K) = 6·140 (5) Å.
‡ $R(I) = \sum|I_o - I_c|/\sum I_o$.
§ Taken from Table 5 (refinement *C*5; H constrained to C).

(1975*d*) are considerably higher than those adopted by Sugawara & Kanda (1952).

Molecular motions in cubic and in orthorhombic acetylene have been the subject of extensive studies by Raman, far IR, and PMR (or DMR) techniques. Only the results for the cubic phase are given here. For this phase, Raman spectra reveal the existence of librational modes with low frequencies of 22–67 cm^{-1} (Ito, Yokoyama & Suzuki, 1970). In addition to these strong librational motions, a cooperative reorientation of the molecules occurs at all temperatures (Albert & Ripmeester, 1972; Perlman, Gilboa & Ron, 1972, 1973; Scheie, Peterson & O'Reilly, 1973). The spectral measurements do not give conclusive evidence about the directions of the rotational axes. All authors assume, however, that the time spent in jumping is negligible compared to the time spent on the equilibrium sites, in agreement with the neutron and X-ray studies, which show preferred positions for the molecules in the solid state. Reorientations of the molecules cause the observed reduction in intensity and the broadening of the far IR bands associated with the translational lattice modes (Schwartz, Ron & Kimel, 1969, 1971). Near the melting point, self-diffusion of the molecules starts to take place. The strong molecular motion in the crystal is consistent with the low melting entropy of acetylene (4·6 e.u.) and with the classification of acetylene as a globular compound (Timmermans, 1961).

3. Crystal growth

3.1. *General*

For our experiments acetylene gas (dissolved in acetone), commercially available from Hoek–Loos, with a quoted purity greater than 99% was used. *Via* a cold (200 K) spiral (for condensation of impurities), the gas was transported into capillary tubes as described by van Nes & van Bolhuis (1978). The crystals were grown *in situ* on a CAD-4 diffractometer in a stream of cold nitrogen gas. The same cooling equipment was used as in the ethane experiment (van Nes & Vos, 1978). In order to obtain temperatures higher than the transition temperature T_o of 133 K, the nitrogen gas was strongly heated by a very long thoroughly twisted heating wire mounted in the Dewar tube. Temperatures, which were defined relative to T_o, were measured with a Chromel–Alumel thermocouple, and were kept stable within 0·1 K.

3.2. *Cubic modification*

Single crystals had been obtained earlier by Sugawara & Kanda (1952) from liquid acetylene at a pressure higher than 1 atm (10^5 Pa) (note that for atmospheric pressure acetylene has a direct gas–solid-state transition). During our experiments liquid acetylene was observed in a very narrow temperature interval.

In order to keep the thermal motion of the molecules as small as possible, it is necessary to collect the acetylene data just above T_o. Various attempts were made to grow single crystals of high quality at this temperature. However, under these conditions no single crystals could be grown with a mosaic spread m smaller than 0·7°. On the other hand, crystals with $m < 0·2°$ were very easy to obtain at temperatures just below the melting point (192 K), but subsequent lowering of the temperature down to slightly above T_o made $m > 0·7°$ in all cases. Finally, for the collection of the data set used for the refinements presented in the present paper (set 1977 in Table 2), a crystal was grown directly at the temperature of the diffraction experiment (141 K) with method (*b*) described by van Nes & van Bolhuis (1978). A clear transparent crystal

was obtained with a maximum reflexion width of 0·7°, determined by an ω scan with a narrow counter slit. In addition to the single crystal, the spherical end of the capillary ($\varnothing$ = 0·587 ± 0·004 mm) contained a tiny misorientated crystallite. As far as we could detect from the reflexion profiles, this crystallite has not affected the accuracy of the reflexion intensities.

During the data collection, the colourless crystal became deep red after about two days. This phenomenon was observed for several crystals. After sublimation of such an acetylene crystal, part of the wall of the capillary sphere remained covered with a thin red layer. This layer has tentatively been considered as polymerized acetylene, as polymerization has been reported to take place at 77 K under irradiation with γ rays (Tabata, Saito, Shibano, Sobue & Oshima, 1964).

3.3. *Orthorhombic modification*

For orthorhombic acetylene only powder studies (Table 1), and no single-crystal experiments have been described in the literature. Our attempts to grow single crystals with $m < 1·0°$ for the orthorhombic phase of acetylene were successful only once. After determination of the cell constants, which were consistent with the values reported by Koski (1975*c*), the crystal sublimed because of an instability in an old version of the cooling equipment. In general, the crystals became opaque during the phase transition.

4. Data collection and comparison of data sets

4.1. *Comparison of data sets*

Characteristic features of three data sets collected in 1975, 1976 and 1977 are given in Table 2. In all cases the measurements were carried out with the $\theta/2\theta$ scan technique on an Enraf–Nonius CAD-4 diffractometer with Mo radiation. The intensities were calculated as the averages of the equivalent reflexion intensities in space group *Pa*3. Comparison of the data sets shows that, especially for the high-order reflexions, the intensities of the 1977 set are the largest. The increases in the intensities are mainly due to use of a larger crystal and a lower temperature, whereas substitution of the Zr filter by a graphite monochromator plus an Al rod has reduced the standard deviations. Because of the correlation effects to be discussed in § 5 and § 7, no advanced refinements have been performed with the 1975 and 1976 sets. Further details of the data collection and refinement results will therefore be given for the 1977 set only.

4.2. *The* 1977 *data set*

Details concerning the monochromatized X-ray beam (wavelength spread, homogeneity) are reported by van Nes & Vos (1978; ethane experiment). The set-up of the monochromatizing device is described by Helmholdt & Vos (1977); in the present work, the glass rod of their Fig. 1 was replaced by an Al rod. Values for the a axis at different temperatures (see Table 1) were determined from θ, φ, ω and κ setting angles measured on the CAD-4 diffractometer. In general one set of 24 reflexions was used, but at the temperature of the intensity measurement (141 K), three sets were taken. At this temperature a = 6·091 (3) Å and D_x = 0·765 Mg m^{-3} for Z = 4.

Table 2. *Data sets for cubic acetylene* (*see text*)

Year		1975	1976	1977
Crystal shape		Cylinder	Sphere	Sphere
Crystal volume (mm^3)		*ca* 0·053	0·105	0·106
Temperature (K)		*ca* 160	170	141
a (Å)		6·127 (3)	6·131 (2)	6·091 (3)
Mosaic spread (°)		<0·8	<0·4	<0·7
X-ray tube (mA)		20	20	32
Filter device		Zr	Graphite + Al	Graphite + Al
Number of reflexions with $I \geq 3\sigma(I)$		67	88	106
C≡C (Å)*		1·137 (7)	1·141 (5)	1·153 (4)
C–H (Å)*		0·91 (5)	1·02 (3)	0·99 (2)
$R(F)$*		0·091	0·061	0·046
$h\,k\,l$	sin θ/λ(Å^{-1})		I (net, relative)	
1 1 1	0·14	11629	29384	34870
2 0 0	0·16	6006	16342	19636
2 1 0	0·18	630	1745	2322
8 0 0	0·66	5	6	25
9 1 1	0·75	1	1	5

* From conventional refinements with $w(F) = 1$; $R(F) = [\sum(F_o - F_c)^2/\sum F_o^2]^{1/2}$.

The net intensities were obtained as described for ethane (van Nes & Vos, 1978). For 2262 reflexions lying in about one half of reciprocal space with $(\sin\theta/\lambda)_{max}$ = 0·90 Å^{-1}, intensities at two ψ values were collected, scan range (1·50 + 1·00 tan θ)° plus 25% background region on both sides, slit width 1·99°. A correction of ±1·0% deduced from the variations of a set of four reference reflexions (measured every 30 min) was made to account for changes in the intensity of the primary beam and/or possible changes in the reflecting power of the crystal. Comparison of the intensities of the equivalent reflexions and consideration of the systematic absences confirm the symmetry *Pa*3 found by Sugawara & Kanda (1952). Four observed intensities with deviations larger than $6\sigma_{count}$ (individual I) from the corresponding average values were removed from the set. From the remaining 4518 intensities, average values $\bar{I}(\mathbf{H})$ were calculated for all 237 independent reflexions up to $\sin\theta/\lambda$ = 0·90 Å^{-1}. The standard deviation in the average values was taken as

$$\sigma[\bar{I}(\mathbf{H})] = \left\{\sum_{\mathbf{H},i} [I(\mathbf{H}_i) - \bar{I}(\mathbf{H})]^2/[n(\mathbf{H})][n(\mathbf{H}) - 1]\right\}^{1/2},$$

where $\mathbf{H}_i$ is an individual reflexion, and $n(\mathbf{H})$ the number of equivalent reflexions in set **H**. Inspection of the average intensities revealed that for $0{\cdot}80 < \sin\theta/\lambda < 0{\cdot}90$ Å^{-1}, there are only four reflexions with $\bar{I} > 3\sigma(\bar{I})$. It was therefore decided to consider for the refinement of the structure only the 164 reflexions up to $\sin\theta/\lambda = 0{\cdot}80$ Å^{-1} among which there are 102 reflexions with $\bar{I} > 3\sigma(\bar{I})$ and 26 reflexions with $\bar{I} \leq 0$. For this set of 164 reflexions, the internal consistency factor is:

$$R(I) = \left\{\sum_{\mathbf{H},i} [I(\mathbf{H}_i) - \bar{I}(\mathbf{H})]^2 / \sum_{\mathbf{H},i} I^2(\mathbf{H}_i)\right\}^{1/2} = 0{\cdot}028.$$

In addition to the I values, for the reflexions with positive net intensities, $|F|$ values were calculated after correction for Lorentz and polarization effects, while for negative I values, $|F| = 0$ was taken. The standard deviations $\sigma(|F|)$ were estimated from $\sigma(\bar{I})$.

5. Geometrical description of the structure and conventional refinements

As mentioned before, acetylene at 141 K crystallizes in space group $Pa3$, $a = 6{\cdot}091\,(3)$ Å, $Z = 4$. The molecules lie at special positions with symmetry $\bar{3}$ (Fig. 1, *ORTEP*; Johnson, 1970), implying that there is only one independent C–H unit. For a geometrical description of the structure, only the values for C≡C and C–H are required. We assumed that the bond lengths in the crystal are not significantly different from those in the gas phase and have adopted the r_e values C≡C = 1·2033 (2), C–H = 1·0605 (3) Å calculated from Raman spectra of acetylene in the gas phase (Fast & Welsh, 1972). Fig. 2 shows that no short intermolecular distances occur, indicating that the structure at 141 K is loosely packed which is also apparent from the considerable thermal motion found by spectral work (§ 2).

In a conventional spherical refinement only the x coordinate and the U values $U_\parallel$ and $U_\perp$ parallel and perpendicular to the [111] direction need to be varied for each of the two independent atoms. Refinements on both I and $|F|$ were performed with the spherical part of the program *VALRAY* (Stewart, 1974). In both cases only up to first-order terms were considered in the Taylor series for I_c and $|F_c|$ respectively, and the weights in $|F|$ were taken as $w(|F|) = |F|^2(\mathrm{Lp})^{1/2} w(I)$, with $w(I) = 1/\sigma^2(\bar{I})$. Therefore the only difference between the two types of refinements is that for reflexions with negative observed intensities, the observed intensity is used in the I refinements, whereas in the $|F|$ refinement $|F_o| = 0$. No significant differences were obtained for corresponding parameters. The scattering factor for C was taken from Cromer & Mann (1968) and that for H from Stewart, Davidson & Simpson (1965). The full-angle refinement, with reflexions up to $\sin\theta/\lambda = 0{\cdot}80$ Å^{-1}, gave C≡C = 1·149 (3), C–H = 0·964 Å, $R_w(I) = 0{\cdot}054$, $R_w(|F|) = 0{\cdot}028$ with $R_w(Y) = [\sum w(Y_o - Y_c)^2 / \sum wY_o^2]^{1/2}$ with Y either I or $|F|$. As usual, the parameters obtained for H are not very reliable, and it was therefore decided to constrain H to C in all further refinements.

No reliable C parameters could be obtained by high-order refinements. Strong correlation (0·98 for $\sin\theta/\lambda > 0{\cdot}55$ Å^{-1}) exists between the overall temperature factor parameter and the scale factor, and the value calculated for C≡C depends quite strongly on the intensity set used: for $\sin\theta/\lambda > 0{\cdot}60$ Å^{-1} the C≡C length is 0·007 Å larger than for $\sin\theta/\lambda > 0{\cdot}55$ Å^{-1}. Neither can reliable C parameters be deduced from Koski's (1975*d*) neutron diffraction work, as this is not sufficiently accurate for this purpose.

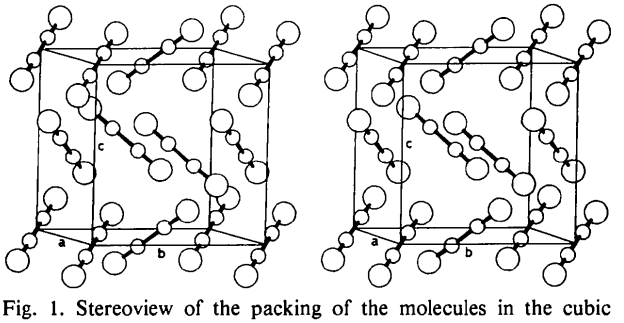

Fig. 1. Stereoview of the packing of the molecules in the cubic phase of acetylene.

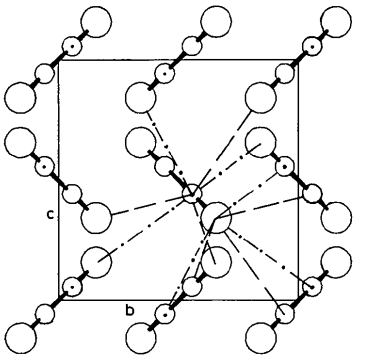

Fig. 2. C_2H_2 structure seen along **a**. For one independent C–H unit all non-bonding distances shorter than the sum of the relevant van der Waals radii [r(C) = 1·7, r(H) = 1·2 Å (Pauling, 1960)] plus 0·4 Å are given; dashed lines are 3·05 Å and chain-dotted lines 3·26 Å.

6. Models for advanced refinements

6.1. *Description of thermal motion, constraints*

The translational and librational motions of the C_2H_2 molecule, as well as its internal vibrations, have been assumed to be harmonic. The non-linear character of

the librational motion has been accounted for by including third and fourth cumulant terms in the temperature factor (Johnson, 1969). The expressions for these cumulants have been derived starting from formula 6.31 of Willis & Pryor (1975) (in which $L_{11}Q_2^2Q_3$ and $L_{22}Q_1^2Q_3$ have to be replaced by $L_{11}^2Q_2^2Q_3$ and $L_{22}^2Q_1^2Q_3$). There are two (equivalent) libration axes perpendicular to the $\bar{3}$ axis. For a libration of $L(\text{rad}^2)$ around each of these axes, the contribution of the independent C atom to the structure factor $F(\mathbf{S})$ reads

$$F(\mathrm{C};\mathbf{S}) = f(\mathrm{C};\mathbf{S}) \times c_1 \times \Delta c_1 \times c_2 \times c_3 \times c_4, \quad (1)$$

with, for $\mathbf{S} = \mathbf{H}$,

$$c_1 = \exp[2\pi i r(\mathrm{C})\, a^*(h + k + l)/\sqrt{3}],$$

$$\Delta c_1 = \exp[-2\pi i r(\mathrm{C})\, a^*\, L(h + k + l)/\sqrt{3}],$$

$$c_2 = \exp\{-2\pi^2 a^{*2}[(h^2 + k^2 + l^2)(U_{\parallel} + 2U_{\perp}) + (2hk + 2hl + 2kl)(U_{\parallel} - U_{\perp})]/3\},$$

$$c_3 = \exp[-8\pi^3 i r^3(\mathrm{C})\, a^{*3} L^2(h^3 + k^3 + l^3 - 3hkl)/3\sqrt{3}],$$

$$c_4 = \exp[16\pi^4 r^4(\mathrm{C})\, a^{*4} L^3(h^4 + k^4 + l^4 + h^3k + h^3l + hk^3 + hl^3 + k^3l + kl^3 - 3h^2kl - 3hk^2l - 3hkl^2)/9].$$

$r(\mathrm{C}) = \frac{1}{2}l(\mathrm{C}{\equiv}\mathrm{C})$ gives the distance of C to the molecular centre. A similar expression can be derived for H. In the case of linear harmonic motions, $F(\mathrm{C};\mathbf{S}) = f(\mathrm{C};\mathbf{S}) \times c_1 \times c_2$. Due to the presence of the libration, the effective $x(\mathrm{C})$ coordinate as found in the refinement is given by

$$x(\mathrm{C}) = [r(\mathrm{C})\, a^*/\sqrt{3}](1 - L). \quad (2)$$

In all refinements of § 7, we constrained c_3 and c_4 to $x(\mathrm{C})$ by use of (2) with $r(\mathrm{C}) = \frac{1}{2}l(\mathrm{C}{\equiv}\mathrm{C}) = 0{\cdot}6017\,(1)$ Å (Raman value). For the higher powers of L the relation $(L_0 + \Delta L)^n = L_0^n + n\Delta L$ was applied, since the program considers linear constraints only. Care was taken that towards the end of the refinement a value close to the final value of L was used for L_0.

Constraining H *to* C

The effective $x(\mathrm{H})$ coordinate is given by relation

$$x(\mathrm{H}) = x(\mathrm{C}) + [r(\mathrm{H}) - r(\mathrm{C})]\,[1 - L]\, a^*/\sqrt{3}; \quad (3)$$

Table 3. $U_{\parallel}$ *(int.) and* $U_{\perp}$ *(int.)* $(10^{-4}$ Å$^2)$ *for* C *and* H *in* C_2H_2

Vibration	$U_{\parallel}$(C)	$U_{\perp}$(C)	$U_{\parallel}$(H)	$U_{\perp}$(H)
Σ_g^+	3·21	–	3·21	–
Σ_u^+	0·37	–	52·17	–
Π_g	–	4·49	–	83·3
Π_u	–	0·73	–	103·0
Total	3·58	5·21	55·38	186·3

for $r(\mathrm{H})$ the Raman value $\frac{1}{2}l(\mathrm{C}{\equiv}\mathrm{C}) + l(\mathrm{C}{-}\mathrm{H}) = 1{\cdot}6622\,(4)$ Å was taken. The temperature factor for H was obtained from that of C by accounting for the internal (linear) vibrations, the molecular translation **T** and libration **L**. The $U(\text{int.})$ values due to internal vibrations were calculated from Meisingseth & Cyvin (1961) by use of the Wilson (1941) approximation. The calculated values are listed in Table 3. This gives the constraints

$$U_{\parallel}(\mathrm{H}) = U_{\parallel}(\mathrm{C}) + [U_{\parallel}(\text{int., H}) - U_{\parallel}(\text{int., C})] + \tfrac{1}{2}L^2[r^2(\mathrm{H}) - r^2(\mathrm{C})], \quad (4)$$

$$U_{\perp}(\mathrm{H}) = U_{\perp}(\mathrm{C}) + [U_{\perp}(\text{int., H}) - U_{\perp}(\text{int., C})] + L[r^2(\mathrm{H}) - r^2(\mathrm{C})]. \quad (5)$$

The above procedure implies that in addition to scale and populations, only three independent variables, specified as $x(\mathrm{C})$, $U_{\perp}(\mathrm{C})$ and $U_{\parallel}(\mathrm{C})$, had to be refined.

6.2. *Description of bonding effects*

Major branches of approach for the description of bonding effects are: (1) representation of 'extra' density in lone-pair regions and on chemical bonds by additional atoms (Hellner, 1977), (2) addition of spherical and aspherical deformation functions to unperturbed SCF atoms (deformation analysis; Dawson, 1967; Hirshfeld, 1971), (3) use of unperturbed cores and modified valence functions (valence analysis; Stewart, 1976; Coppens, 1975, and references therein). We have carried out a valence analysis with restricted radial density basis functions (Bentley & Stewart, 1976; Stewart, 1976) by use of *VALRAY* (Stewart, 1974).

In the valence analysis the total (dynamical) density distribution $\rho(\mathbf{r})$ is assumed to be the sum of the densities of the pseudo atoms p (centred at the same position as the 'real' atoms) in the cell

$$\rho(\mathbf{r}) = \sum_p \rho_p(\mathbf{r}_p),$$

with $\mathbf{r}_p = \mathbf{r} - \mathbf{R}_p$ and $\mathbf{R}_p$ the equilibrium position of atom p, and

$$\rho_p(\mathbf{r}_p) = \mathrm{Pop}_p(\text{core})\, \rho_p(\text{core},r_p) + \sum_{l,m=0}^{l} C_p^e(l,m) \times \mathrm{Pop}_p^e(l,m)\, \rho_p(l,r_p)\, P_l^m(\cos\theta_p) \cos m\varphi_p + \sum_{l,m=1}^{l} C_p^o(l,m)\, \mathrm{Pop}_p^o(l,m)\, \rho_p(l,r_p) \times P_l^m(\cos\theta_p) \sin m\varphi_p, \quad (6)$$

where $\rho_p(\text{core},r_p)$ is a normalized SCF density function for p. A deviation of $\mathrm{Pop}_p(\text{core})$ from the free-atom core population, say by an amount $-q_p$, is not considered as a perturbation of the core, but as a

Table 4. *Dipole and quadrupole functions applicable for* C_2H_2

Populations are given by Pop(1,0) and Pop(2,0). Pop(1,0) is positive for electron shifts away from the molecular centre, Pop(2,0) is positive for concentration of electrons around the molecular axis. q is the direction cosine of the Bragg vector relative to the C≡C direction.

$C(1,0)\text{Pop}(1,0)\, P_1^o(\cos\theta) = 4 \times \text{Pop}(1,0) \times q$
$C(2,0)\text{Pop}(2,0)\, P_2^o(\cos\theta) = 3\sqrt{3} \times \text{Pop}(2,0) \times 3(q^2 - \frac{1}{3})/2$

modification of the monopole valence function, $\rho_p(0,r_p)$, in this case of magnitude $[q_p/\text{Pop}_p(0,0)] \times [\rho_p(0,r_p) - \rho_p(\text{core},r_p)]$ (Bentley & Stewart, 1976; Stewart, 1976). $P_l^m(\cos\theta_p)\cos m\varphi_p$ and $P_l^m(\cos\theta_p) \times \sin m\varphi_p$ are unnormalized, associated Legendre functions; r_p, θ_p and φ_p are polar coordinates corresponding to $\mathbf{r}_p$. Multipole functions applicable to the C_2H_2 molecule are given in Table 4. The functions $\rho_p(l,r_p)$ are radial density functions which, in principle, depend on l. The factors $C_p^e(l,m)$ and $C_p^o(l,m)$ in formula (6) are normalization constants. For monopole terms with $l = m = 0$ the constant $C_p^e(0,0)$ is chosen such that $\text{Pop}_p(0,0)$ is the population of the monopole function, thus

$$C_p^o(0,0) \int \rho_p(0,r_p)\, P_0^o\, d\mathbf{r} = 1.$$

For $l > 0$ where the terms integrate to zero, we have chosen $C_p^e(l,m)$ and $C_p^o(l,m)$ such that $\text{Pop}_p(l,m)$ gives the number of electrons transferred from the total negative to the total positive part of the function (Price & Maslen, 1978); thus for $C_p^e(l,m)$

$$C_p^e(l,m) \int |\rho_p(l,r_p)\, P_l^m(\cos\theta_p)\cos m\varphi_p|\, d\mathbf{r}_p = 2.$$

6.3. *Scattering factors*

The generalized scattering factor of atom p is the Fourier transform of (6) and reads

$$\begin{aligned} f_p(\mathbf{S}) = \text{Pop}_p(\text{core})\, f_p(\text{core},S) &+ \sum_{l,m=0}^{l} C_p^e(l,m) \\ &\times \text{Pop}_p^e(l,m)\, i^l\, f_p(l,S)\, P_l^m(\cos\theta_S)\cos m\varphi_S \\ &+ \sum_{l,m=1}^{l} C_p^o(l,m)\, \text{Pop}_p^o(l,m)\, i^l f_p(l,S) \\ &\times P_l^m(\cos\theta_S)\sin m\varphi_S, \end{aligned} \tag{7}$$

with $f_p(l,S)$ the Fourier Bessel transform of $\rho_p(l,r_p)$,

$$f_p(l,S) = 4\pi \int_0^\infty \rho_p(l,r_p)\, j_l(Sr_p)\, r_p^2\, dr_p, \tag{8}$$

where $j_l(Sr_p)$ is an lth-order spherical Bessel function.

For all refinements of § 7 the scattering factor for the C core was derived from the SCF (^3P) wavefunction of Clementi (1965), but for the valence electrons three types of scattering factors have been used.

(*A*) Variable-ζ scattering factors (§7.2; Table 5, series *A*). $\rho_p(l,r_p)$ is written as (Stewart, 1976)

$$\rho_{p,n_p}(r_p) = (4\pi)^{-1}[(2\zeta_p)^{n_p+3}/(n_p+2)!]\, r_p^{n_p} \exp[-2\zeta_p r_p], \tag{9}$$

where n_p is a discrete (integer) variable and ζ a continuous variable. For all multipoles on the same atom ζ_p is shared. The n_p values taken are $n(\text{H}) = 0$, 1, 2 for monopole ($l = 0$), dipole ($l = 1$) and quadrupole ($l = 2$) respectively and $n(\text{C}) = 2$ for the monopole up to the quadrupole and $n(\text{C}) = 3$ for the octopole function. The quality of the (H like) STO type function (9) has been discussed by Bentley & Stewart (1976) and by Stewart (1977).

(*B*) Fixed-ζ scattering factors (§ 7.3; Table 5, series *B*). In this case the radial function (9) is used with ζ(H) fixed at 1·12 and ζ(C) at 1·525. According to Bentley & Stewart (1976), STO functions having these ζ values, project into theoretical SCF densities best for 'molecules' like C=O and C—H. As this is especially true for $\text{Pop}_C(\text{core}) = 2{\cdot}1$, or $q_C = -0{\cdot}1$ (§ 6.2), in one of the 'ζ fixed scattering factor' refinements $\text{Pop}_C(\text{core})$ was fixed at 2·1.

(*C*) SCF scattering factors (§ 7.4; Table 5, series *C*). f(H) is called f(H,pol) and is taken from Stewart, Bentley & Goodman (1975; Table III). The scattering factor for C is called $f(\text{C},^3P)$ and is deduced from the SCF(^3P) Clementi wavefunction.

In Fig. 3, ζ scattering factors for C are compared with the ^3P curve. The ζ values taken are 1·52 (see

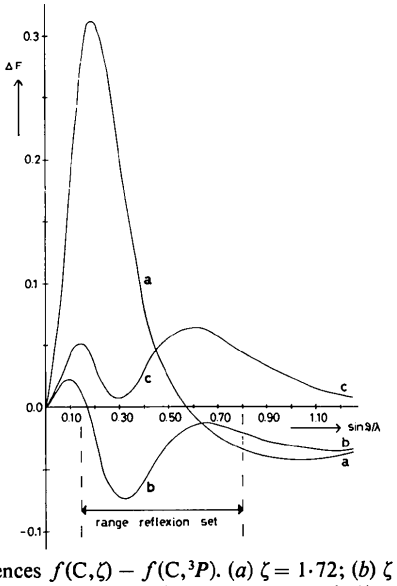

Fig. 3. Differences $f(\text{C},\zeta) - f(\text{C},^3P)$. (*a*) $\zeta = 1{\cdot}72$; (*b*) $\zeta = 1{\cdot}525$; (*c*) $\zeta = 1{\cdot}525$ with $\text{Pop}_C(\text{core}) = 2{\cdot}10$ and $\text{Pop}_C(0,0) = 3{\cdot}90$.

Table 5. *Refinements with different types*

Numbers in parentheses are the estimated standard deviations in the last digits; constrained parameters are indicated with a hyphen explanation of other parameters see text.

Number	Type	N_v	$R_w(I)$ (%)	GOF	f(C, S)	f(H, S)[1]	K	x(C) × 10^5	C≡C (Å)[2]	Pop(core)[3]
*A*1	*s*	7	4·93	5·21	1·63 (1)	1·45 (10)	9·19 (20)	5468 (7)	1·154 (2)	2·00 (–)
*A*2	*s*	8	4·44	4·72	1·65 (3)	1·51 (9)	9·08 (26)	5457 (7)	1·151 (2)	2·00 (–)
*A*3	*dq*	11	1·76	1·89	1·69 (1)	0·92 (3)	8·94 (10)	5608 (9)	1·183 (2)	2·00 (–)
*A*4	*dq*	10	1·77	1·89	1·67 (1)	0·98 (2)	9·08 (9)	5580 (–)	1·177	2·00 (–)
*A*5[5]	*dq*	11	0·88[5]	1·98	1·68 (2)	0·92 (3)	9·01 (12)	5604 (9)	1·182 (2)	2·00 (–)
*A*6[6]	*dq*	11	2·48[6]	0·88	1·77 (4)	0·88 (7)	8·84 (34)	5647 (23)	1·192 (5)	2·00 (–)
*B*1	*s*	5	5·60	5·88	1·525	1·12	9·66 (12)	5472 (9)	1·155 (2)	2·10 (–)
*B*2	*s*	6	5·15	5·43	1·525	1·12	9·81 (13)	5462 (8)	1·152 (2)	2·00 (–)
*B*3	*dq*	9	2·16	2·30	1·525	1·12	10·00 (6)	5544 (7)	1·170 (2)	2·00 (–)
*B*4	*dq*	10	1·92	2·05	1·525	1·12	9·92 (5)	5562 (6)	1·174 (1)	2·00 (–)
*B*5	*dq*	11	1·90	2·04	1·525	1·12	9·92 (5)	5555 (8)	1·172 (2)	2·00 (–)
*C*1	*s*	5	5·74	6·03	^3P	pol	9·58 (14)	5471 (9)	1·154 (2)	2·00 (–)
*C*2	*s*	6	5·05	5·32	^3P	pol	9·15 (16)	5459 (8)	1·152 (2)	2·00 (–)
*C*3	*dq*	9	1·93	2·06	^3P	pol	9·41 (6)	5554 (6)	1·172 (1)	2·00 (–)
*C*4	*dq*	10	1·73	1·85	^3P	pol	9·40 (6)	5568 (6)	1·175 (1)	2·00 (–)
*C*5	*dq*	11	1·70	1·82	^3P	pol	9·36 (6)	5585 (7)	1·178 (2)	2·00 (–)

(1) For ζ scattering factor, ζ values (a.u.) are given. (2) Including librational shortening. (3) See § 7.1. (4) Extinction parameter

above) and 1·72 a.u. ('standard molecular value', obtained from energy minimization for C in molecules; Hehre, Stewart & Pople, 1969). Considerable differences occur even in the high-order part. The present $f(C;^3P)$ curve is almost identical with that of Cromer & Mann (1968) applied in § 5: deviations are less than 0·4% for $\sin\theta/\lambda < 0{\cdot}35$ Å^{-1} and less than 0·1% for higher $\sin\theta/\lambda$ values.

7. Spherical and aspherical refinements with constraints

7.1. *The program VALRAY*

Before the start of our refinements the program *VALRAY* (Stewart, 1974) was adapted to *I* refinements and to the possibility of using linear constraints and higher cumulants (Johnson, 1969) by van der Wal (1978). $R_w(Y)$ with $Y = I$ or $|F|$ is defined in § 5. The least-squares functions minimized are

$$Q(Y) = \sum w(Y_o)\,[Y_o(\mathbf{H}) - K(Y)\,Y_c(\mathbf{H})]^2,$$

with $w(Y_o) = 1/\sigma^2(Y_o)$, $K(I) = K^2$ and $K(|F|) = K$. The goodness of fit is defined as

$$\mathrm{GOF} = \{\sum w[Y_o(\mathbf{H})][Y_o(\mathbf{H}) - Y_c(\mathbf{H})]^2/(N_o - N_v)\}^{1/2}.$$

N_o and N_v are the number of observed independent intensities and the number of variables respectively. For the present work $N_o = 164$.

The program *VALRAY* refers the scale factor K to the cores, for which fixed populations are taken, and considers the quantities $K \times \mathrm{Pop}(l,m)$ for the populations of the valence electrons. Apart from the refinements *A*1, *B*1 and *C*1 (Table 5), the sum of the monopole populations has not been constrained to the total number of electrons n, as, due to the strong correlations (§ 7.2–7.5), the $\mathrm{Pop}_p(0,0)$ values need not be interpreted as the number of valence electrons at p. Normalized populations can be obtained by multiplying $\mathrm{Pop}_p(\mathrm{core})$ and $\mathrm{Pop}_p(l,m)$ by a factor η obtained from the relation

$$\eta\left[\sum_p \mathrm{Pop}_p(\mathrm{core}) + \sum_p \mathrm{Pop}_p(0,0)\right] = n.$$

At the same time the scale factor K must be divided by η.

7.2. *Refinements with variable-ζ scattering factors*

In Table 5, the results of 'ζ-variable' refinements on *I* are given in rows *A*1 to *A*4 and the results of two refinements on $|F|$ in rows *A*5 to *A*6. Both spherical (*s*), and aspherical refinements including additional dipole and quadrupole functions (indicated by *dq*), were performed. In *A*1 the total population has been constrained at 7 (for one H and one C). For *A*2, with no restriction for the total population, the agreement between I_o and I_c is considerably better than for *A*1. The most noticeable feature in this series of refinements is the strong

of scattering factor (series A, B, C;§ 6.3)

between parentheses, fixed ζ's, x(C) and Pop(core)'s are not followed by parentheses. H is constrained to C according to § 6.1. For

C					H					
Pop(0,0)	Pop(1,0)	Pop(2,0)	$U_{\parallel} \times 10^4$	$U_{\perp} \times 10^4$	Pop(0,0)	Pop(1,0)	$U_{\parallel}(-) \times 10^4$	$U_{\perp}(-) \times 10^4$	ΔU(H)	y(ext.)[4]
4·34 (5)			516 (11)	519 (10)	0·66 (–)		593	1686		
4·38 (12)			511 (13)	515 (12)	0·73 (5)		584	1731		
3·98 (6)	–0·19 (1)	0·36 (2)	378 (7)	579 (5)	1·13 (6)	–0·21 (3)	438	1160		
3·99 (5)	–0·15 (1)	0·36 (2)	385 (7)	584 (5)	1·01 (4)	–0·15 (1)	447	1283		
3·97 (5)	–0·18 (1)	0·36 (2)	380 (8)	582 (6)	1·10 (5)	–0·20 (3)	440	1178		
3·74 (10)	–0·26 (3)	0·29 (5)	390 (18)	577 (15)	1·26 (16)	–0·35 (8)	446	992		
4·03 (3)			578 (9)	543 (7)	0·87 (–)		650	1697		
4·36 (6)			552 (9)	532 (8)	0·87 (3)		625	1727		
4·00 (3)	–0·08 (1)	0·40 (2)	430 (7)	616 (5)	0·67 (2)	–0·06 (1)	495	1467		
4·20 (3)	–0·11 (1)	0·38 (2)	430 (6)	608 (4)	0·68 (2)	–0·07 (1)	493	1382		0·85
4·22 (4)	–0·09 (2)	0·39 (2)	429 (7)	609 (4)	0·65 (3)	–0·05 (2)	493	1413	–71	0·86
4·13 (3)			558 (10)	526 (8)	0·87 (–)		630	1683		
4·83 (5)			523 (10)	511 (8)	0·94 (3)		596	1719		
4·38 (3)	–0·12 (1)	0·39 (2)	410 (7)	599 (4)	0·75 (2)	–0·19 (3)	474	1407		
4·53 (3)	–0·07 (1)	0·36 (2)	409 (6)	592 (4)	0·77 (2)	–0·22 (2)	473	1341		0·88
4·52 (3)	–0·19 (2)	0·34 (2)	413 (6)	588 (4)	0·85 (3)	–0·31 (4)	477	1265	141	0·87

for reflexion 111 defined as $I_c^{ext} = I_c y$. (5) Refinement on $|F|$, comparable with $A3$; $R_w(F)$ is given. (6) As $A5$, but $w = 1$.

decrease in $R_w(I)$ from 4·44% ($A2$) to 1·76% ($A3$) by the introduction of the dipole and quadrupole functions. In the spherical refinement $A2$, deviations from spherical symmetry of the (static) atoms, especially the quadrupole-type distortion, are compensated by systematic errors in the thermal parameters. This is seen from the fact that for $A2$ $U_{\parallel}(\mathrm{C}) \simeq U_{\perp}(\mathrm{C})$, while for $A3$ $U_{\parallel}(\mathrm{C}) < U_{\perp}(\mathrm{C})$. For the *dq* refinement $A3$, ζ(C) lies close to the ζ(C) value of 1·67 found for C_2H_2 by Hehre, Stewart & Pople (1969) (energy minimization with minimum basis set), whereas ζ(H) lies close to the ζ(H) value of a free H atom and is lower than the theoretical optimum ζ(H) value of 1·31.

No significant improvement of $R_w(I)$ was obtained by adding an isotropic extinction parameter to the refinement $A3$, nor by the introduction of a quadrupole on H or an octopole on C.

From Table 6 it can be seen that there is considerable correlation not only between the radial parameters, *e.g.* K, U_{ii}, ζ and $P(0,0)$, but also between the positional parameter x(C) and the dipole population of C. Therefore, refinement $A4$ was carried out to check whether an equally good agreement between I_o and I_c could be obtained with a different position for C. In $A4$ constraining the C position 0·003 Å closer to the inversion centre than in $A3$ results in hardly any change in $R_w(I)$ or in the residual difference density map (maps of $A3$ and $A4$, not given in this paper). This clearly shows that, for instance, the dipole moment at C and the position of C cannot be determined uniquely from the present data.

Finally, two refinements on $|F|$ ($A5$ and $A6$) were carried out to study the difference in results between $|F|$ and I refinements. Weighting schemes $w = 1/\sigma^2(|F|)$ and $w = 1$ were applied in refinements $A5$ and $A6$ respectively, with the same set of variables as in refinement $A3$. As expected (see § 5), the parameter values of $A5$ show good agreement with those of $A3$, but significant changes occur for $w(|F|) = 1$.

The list of I_o and I_c values corresponding to refinement $A3$ is given in Table 7.

7.3. *Refinements with fixed-ζ scattering factors*

Results of refinements with ζ(C) = 1·525 and ζ(H) = 1·12 are given as series B in Table 5. The results of $B1$–$B3$ may be compared directly with those of $A1$–$A3$, apart from the fact that in $B1$ the population $\mathrm{Pop_C(core)}$ is fixed at 2·10 (§ 6.3). For the fixed ζ values the agreement between I_o and I_c is considerably less than for the adjustable ζ values. As expected, the change in scattering factor (Fig. 3) induces changes in other parameters, *e.g.* scale, temperature factors and monopole populations.

Finally, an isotropic extinction parameter (Zachariasen, 1967, 1968), with a $\sin\theta$ correction as given by Becker & Coppens (1974), was introduced ($B4$), resulting in considerable improvement (compare $B3$ and $B4$). Extinction is not thought to be physically real, however, for our crystal with $m = 0·7°$, but the y parameter is used as a modification of the scattering-factor curve.

Table 6. *Elements of the correlation matrix for refinement A3 (see Table 5)*

Correlation coefficients ρ_{ab} with $a \neq b$ larger than 0·70 are underlined.

		C								H		
		K	ζ	x	U_{ii}	U_{ij}	$P(0,0)$	$P(1,0)$	$P(2,0)$	ζ	$P(0,0)$	$P(1,0)$
	K	+1·00	−0·84	−0·47	+0·98	+0·23	+0·64	+0·28	+0·32	+0·54	−0·51	+0·41
	ζ	−0·84	+1·00	+0·52	−0·73	−0·33	−0·91	−0·40	−0·26	−0·58	+0·62	−0·56
	x	−0·47	+0·52	+1·00	−0·45	−0·05	−0·59	−0·90	−0·30	−0·74	+0·70	−0·83
C	U_{ii}*	+0·98	−0·73	−0·45	+1·00	+0·14	+0·52	+0·26	+0·35	+0·52	−0·47	−0·37
C	U_{ij}*	+0·23	−0·33	−0·05	+0·14	+1·00	+0·26	−0·15	−0·75	+0·17	−0·06	−0·04
	$P(0,0)$	+0·64	−0·91	−0·59	+0·52	+0·26	+1·00	+0·53	+0·23	+0·68	−0·75	+0·72
	$P(1,0)$	+0·28	−0·40	−0·90	+0·26	−0·15	+0·53	+1·00	+0·48	+0·65	−0·71	+0·90
	$P(2,0)$	+0·32	−0·26	−0·30	+0·35	−0·75	+0·23	+0·48	+1·00	+0·16	−0·32	+0·42
	ζ	+0·54	−0·58	−0·74	+0·52	+0·17	+0·68	+0·65	+0·16	+1·00	−0·95	+0·84
H	$P(0,0)$	−0·51	+0·62	+0·70	−0·47	−0·06	−0·75	−0·71	−0·32	−0·95	+1·00	−0·89†
	$P(1,0)$	+0·41	−0·56	−0·83	−0·37	−0·04	+0·72	+0·90	+0·42	+0·84	−0·89†	+1·00

* U_{ii} and U_{ij} are taken from the temperature factor $\exp[-2\pi^2(h_i a^{i})(h_j a^{j})\, U^{ij}]$.

† High value due to the fact that x(H) is constrained to x(C).

Table 7. *Observed and calculated intensities for refinement A3*

Each group of six columns contains h,k,l, $100I_o$, $100I_c$, and $100\sigma(I_o)$ respectively.

H K L	IOBS	ICALC	SIGI	H K L	IO	IC	S	H K L	IO	IC	S
1 1 1	422668	438826	4777	5 5 4	11	11	3	7 3 1	93	84	2
2 0 0	238013	234665	2275	5 5 5	12	1	5	7 3 2	59	50	3
2 1 0	28144	27922	115	6 0 0	723	717	5	7 3 3	13	12	3
2 1 1	14715	14771	47	6 0 2	356	362	4	7 3 4	61	59	4
2 2 0	51133	50486	192	6 0 4	18	31	5	7 3 5	-3	1	3
2 2 1	2311	2327	10	6 1 0	239	243	5	7 3 6	7	17	4
2 2 2	14295	14635	92	6 1 1	206	204	3	7 4 1	95	98	2
3 0 2	16131	16128	53	6 1 2	111	112	3	7 4 2	1	0	3
3 1 1	14214	14316	51	6 1 3	661	676	5	7 4 3	6	8	4
3 1 2	114	117	4	6 1 4	-3	2	3	7 4 4	-7	0	3
3 2 1	11324	11234	43	6 1 5	219	225	3	7 4 5	1	5	5
3 2 2	4087	4100	11	6 2 0	365	362	3	7 5 1	0	0	4
3 3 1	1636	1660	8	6 2 1	13	11	3	7 5 2	17	28	3
3 3 2	853	871	4	6 2 2	174	175	3	7 5 3	-2	1	5
3 3 3	72	71	6	6 2 3	51	47	3	7 5 4	24	32	2
4 0 0	727	690	8	6 2 4	14	11	2	7 6 1	9	10	5
4 0 2	520	513	6	6 2 5	29	28	3	7 6 2	11	6	3
4 1 0	2577	2529	11	6 3 0	831	833	5	7 6 3	-9	0	5
4 1 1	1970	1956	8	6 3 1	28	33	2	8 0 0	298	285	6
4 1 2	923	928	6	6 3 2	345	346	6	8 0 2	130	132	3
4 1 3	5096	5091	17	6 3 3	95	92	3	8 0 4	5	5	7
4 2 0	528	513	6	6 3 4	8	4	4	8 1 0	9	7	2
4 2 1	-2	1	4	6 3 5	22	24	3	8 1 1	6	5	3
4 2 2	119	131	4	6 4 0	19	31	4	8 1 2	0	2	3
4 2 3	72	74	4	6 4 1	9	15	2	8 1 3	9	15	4
4 3 0	6264	6325	29	6 4 2	12	11	3	8 1 4	-3	0	3
4 3 1	271	261	4	6 4 3	60	58	3	8 1 5	0	3	4
4 3 2	2611	2596	9	6 4 4	-3	0	2	8 2 0	134	132	3
4 3 3	761	746	4	6 4 5	41	34	4	8 2 1	4	7	3
4 4 0	-5	1	3	6 5 0	276	282	4	8 2 2	62	58	3
4 4 1	10	27	4	6 5 1	9	2	3	8 2 3	31	29	4
4 4 2	6	2	4	6 5 2	108	108	3	8 2 4	-1	1	4
4 4 3	75	67	4	6 5 3	8	7	3	8 2 5	11	16	4
4 4 4	6	2	5	6 5 4	1	0	6	8 3 0	17	20	3
5 0 2	2170	2200	11	6 5 5	7	6	4	8 3 1	-2	0	5
5 0 4	1871	1892	12	6 6 0	2	2	4	8 3 2	9	6	6
5 1 1	161	149	4	6 6 1	4	5	3	8 3 3	2	0	5
5 1 2	-4	4	4	6 6 2	11	2	5	8 3 4	-2	1	4
5 1 3	45	47	3	6 6 3	18	20	3	8 4 0	6	5	5
5 1 4	10	2	3	6 6 4	4	2	6	8 4 1	3	9	4
5 2 1	1835	1826	8	7 0 2	138	152	4	8 4 2	7	1	4
5 2 2	996	997	4	7 0 4	112	124	5	8 4 3	27	34	6
5 2 3	317	303	3	7 0 6	26	14	4	8 5 0	-2	4	4
5 2 4	785	780	4	7 1 1	424	417	4	8 5 1	-1	1	7
5 3 1	40	47	4	7 1 2	8	12	4	8 5 2	-4	1	5
5 3 2	5	6	4	7 1 3	84	84	3	9 0 2	-1	0	7
5 3 3	23	16	3	7 1 4	22	15	2	9 1 1	65	62	4
5 3 4	12	10	3	7 1 5	-1	0	5	9 1 2	-6	3	4
5 4 1	1525	1529	4	7 1 6	-2	4	5	9 1 3	10	10	4
5 4 2	30	26	3	7 2 1	119	122	3	9 2 1	-5	0	5
5 4 3	221	214	2	7 2 2	54	60	3	9 2 2	-3	0	5
5 4 4	17	12	3	7 2 3	18	13	2	9 2 3	0	0	4
5 5 1	-2	6	3	7 2 4	49	45	3	9 3 1	6	10	4
5 5 2	2	6	3	7 2 5	4	3	4	9 3 2	7	12	5
5 5 3	7	0	3	7 2 6	-3	4	4				

In *B*5 another attempt was made to modify the H scattering factor (inclusive of thermal motion) relative to that of C by multiplying the constrained temperature factor of H by $\exp[-8\pi^2\, \Delta U(\mathrm{H}) \sin^2\theta/\lambda^2]$ and refining ΔU(H). Only a small improvement was obtained in this way.

7.4. *Refinements with SCF scattering factors* (^3P *refinements*)

By analogy to the fixed-ζ refinements of series *B*, the refinements of series *C* were also set up with fixed scattering curves, *viz* with $f(\mathrm{C},{}^3P)$ and f(H,pol) (§ 6.3). Refinements *C*1–*C*5 are directly comparable with *B*1–*B*5. Again, introduction of an isotropic extinction parameter gives a marked improvement, whereas only a slight improvement is achieved by the introduction of ΔU(H). For refinement *C*5, the value of $R_w(I)$ is lower than for any of the other refinements.

7.5. *Review of the final refinements*

The final refinements of the series *A*, *B*, and *C*, *viz* *A*3, *B*5, and *C*5, contain the same number of adjustable parameters (N_v). In all cases, two of them are modification parameters of the scattering-factor curves, *viz* ζ(C) plus ζ(H) for *A*3, and y(ext.) plus ΔU(H) for *B*5 and *C*5. The $R_w(I)$ value of *B*5, 1·90%, is considerably higher than the values of 1·76% for *A*3 and 1·70% for *C*5. The results of both *A*3 and *C*5 will be considered in the density analysis of the next section.

The total (unscaled) population deviates more from 7 for *C*5 than for *A*3. This shows that population parameters are not observables, but depend on the types of radial function applied. P(monopoles;H)/P(mono-

poles;C) agrees better with the theoretical SCF calculation of Clementi & Popkie (1972) (C = 6·15, H = 0·85) for *C*5 than for *A*3. Due to the use of the different radial functions, there are differences greater than 3σ between the thermal parameters of *A*3 and *C*5.

8. Electron density distributions

8.1. *Final difference Fourier synthesis* $D_f(\mathbf{r})$

Final difference Fourier maps $D_f(\mathbf{r})$ were calculated for refinement *C*5 [^3P scattering factor for C, f(H,pol.) for H] and refinement *A*3 (ζ scattering factors), both with the full set of 164 reflexions and with the set of 138 reflexions with $I > 0$. In all these four cases standard deviations for arbitrary positions, as estimated from the formula $\sigma(D_f) = V^{-1}\{\sum_{\mathbf{H}}[K^{-1}F_o - F_c \text{ (final model)}]^2\}^{1/2}$, are 0·02 e Å^{-3}. From this value, the standard deviation for general positions on the $\bar{3}$ axis are estimated to be 0·035 e Å^{-3} and that at the origin 0·05 e Å^{-3}. In none of the $D_f(\mathbf{r})$ maps do deviations from zero greater than three times the relevant σ occur. In spite of this, Fig. 4 still shows systematic features along the molecular axis. These are due to the fact that in the difference map the weak high-order reflexions have obtained a higher weight than corresponds with their accuracy. The slope at C in the positive *Z* direction corresponds to the (not significant) positive C shift when in the least-squares refinements the weighting of the reflexions according to their accuracy is replaced by $w(F) = 1$ (Table 5, *A*5 and *A*6). As the effect discussed above results primarily from the very weak reflexions, it was decided to calculate all further maps with the reflexions having $I > 0$.

8.2. *Influence of non-linearity of the librational motion*

An [F_c (final model) − F_c (final model, but $c_3 = c_4 = 1$)] map, with density values varying between −0·01 and +0·01 e Å^{-3}, showed that the influence of the non-linearity of the librational motion (§ 6.1) on the model density is negligibly small. At first sight this result is surprising, as $(\overline{\varphi^2})^{1/2}$ is as large as 8·2 and 7·4° for refinements *C*5 and *A*3 respectively. It can be understood from the small distance of 0·6017 Å between C and the librational axes, because of which c_3(C) and c_4(C) only differ appreciably from 1 for the high-order reflexions. Because of the large thermal motion these reflexions are so weak that introduction of the factors c_3 and c_4 results in only small $|\Delta F_c|$ values.

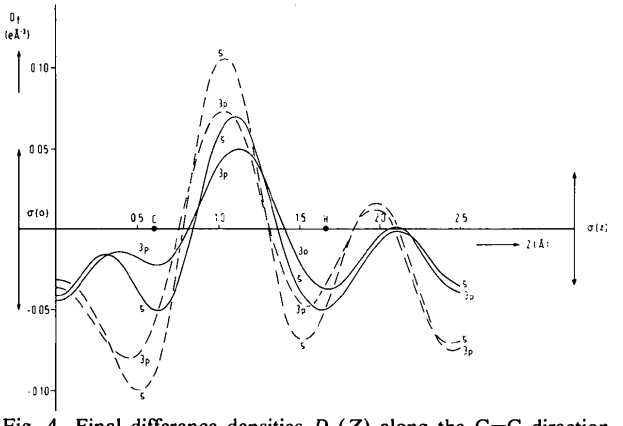

Fig. 4. Final difference densities $D_f(Z)$ along the C≡C direction (indicated as *Z* in this and in following figures) for refinement *C*5 (^3P scattering factors) and refinement *A*3 (ζ scattering factors). Dashed lines for 164, and solid lines for 138 independent reflexions (see text). $\pm\sigma$ values are indicated by vertical arrows, right for general *Z* values, left for $Z = 0$.

8.3. *Filtered and unfiltered deformation maps*

From the final difference maps and the low $R_w(I)$ values of *A*3 and *C*5, it follows that ρ_c(multipole model;**r**) gives a good filtered representation for $K^{-1}\rho_o(\mathbf{r})$. However, because of the correlations discussed in § 7.2 and § 7.5, the U_{ij} values, the monopole populations and *K* are affected by errors which also depend on the radial functions used. Therefore in the difference map

$$D_M(\mathbf{r}) = \rho_c(\text{multipole model};\mathbf{r}) - \rho_c(\text{atoms};\mathbf{r}),$$

with ρ_c(atoms; **r**) based on non-bonded SCF atoms; ρ_c(multipole model;**r**) is likely to correspond to an incorrectly scaled $\rho_o(\mathbf{r})$ map, whereas ρ_c(atoms;**r**) contains incorrect U_{ij} thermal parameters. For the monopole deformations ρ_c(monopoles;**r**) − ρ_c(atoms;**r**) considerable errors are expected, especially at C where they may amount to some 0·3 e Å^{-3}. For the non-monopole deformations the percentage error is approximately equal to the percentage error in *K* and is estimated as 0·03 e Å^{-3} at the centre of C≡C. Because of the uncertainties in the scale factor (and thermal motion) we have chosen to calculate filtered maps without monopole deformations. For the present case the filtered maps are thus defined as

$$\begin{aligned} D_{\text{fi}}(\mathbf{r}) &= \rho_c(\text{multipole model};\mathbf{r}) - \rho_c(\text{monopoles};\mathbf{r}) \\ &= \sum_{\mathbf{H}} [F_c(\text{multipole model};\mathbf{H}) \\ &\qquad - F_c(\text{monopoles};\mathbf{H})] \exp(-2\pi i \mathbf{H}.\mathbf{r}). \end{aligned}$$

For each $D_{\text{fi}}(\mathbf{r})$ map a consistent set of parameters, including the radial functions, is used. The $D_{\text{fi}}(\mathbf{r})$ map based on the model of the ζ refinement will be denoted as $D_{\text{fi}}(\zeta,\mathbf{r})$, and the map for the ^3P refinement as $D_{\text{fi}}(^3P,\mathbf{r})$. In addition to the filtered $D_{\text{fi}}(\mathbf{r})$ maps, unfiltered deformation maps, again with exclusion of monopole deformations, have been calculated as

$$D(\mathbf{r}) = K^{-1}\rho_o(\mathbf{r}) - \rho_c(\text{monopoles};\mathbf{r}),$$

with ρ_c(monopoles;**r**) based on the cores and monopole valence functions with populations as found in the respective refinements.

The unfiltered deformation maps are given in Figs. 5(*a*), (*b*) and 6 and filtered maps in Fig. 5(*c*), (*d*).

The largest difference between the filtered maps for the ^3P and the ζ refinements is found at the centre of C≡C, where $D_{\rm fi}(^3P) = 0{\cdot}60$ and $D_{\rm fi}(\zeta) = 0{\cdot}775$ e Å^{-3}. About 60% of this difference of 0·175 e Å^{-3} can be attributed to the difference between the *C*5 and *A*3 dipole and quadrupole populations for C (Table 5); the remaining 40% may be ascribed to the differences between the (modified) ^3P and ζ radial functions and, for the ζ maps, also to series termination. Both for the ^3P- and ζ-filtered maps the densities at the atoms are close to zero, as the maps are based on quadrupole and dipole functions centred on the atoms only. The small deviations from zero at the atomic positions arise from anisotropic thermal smearing and from contributions of neighbouring atoms.

The (unfiltered) deformation density of Fig. 6 shows six symmetrically related density minima of −0·045 e Å^{-3} (−2·4σ) and six related maxima of +0·07 e Å^{-3} (+3·7σ) at a distance of 1·52 Å from the C≡C bond. The average density in the ring deviates about 0·040 e Å^{-3} from that in the filtered map based on dipole and quadrupole functions, only. The one independent maximum (minimum) may be due to random errors, but it cannot be excluded that it is indicative of a small octopole-type deformation due to intermolecular interactions.

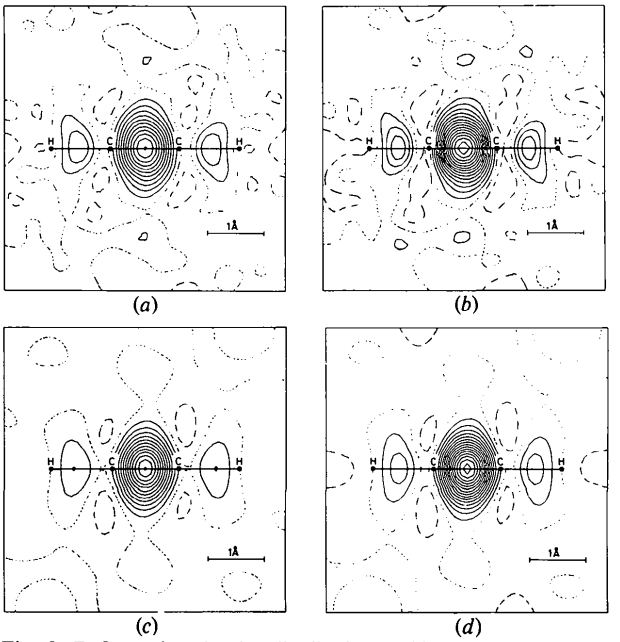

Fig. 5. Deformation density distributions $D(\mathbf{r})$ and corresponding filtered maps $D_{\rm fi}(\mathbf{r})$. A section through the diagonal plane is shown. Contours in this and following figures are at intervals of 0·05 e Å^{-3}. Full lines are positive, short-dashed lines zero and long-dashed lines negative contours. (*a*) D(**r**, 138 reflexions, ^3P); (*b*) D(**r**, 138 reflexions, ζ); (*c*) $D_{\rm fi}$(**r**, 138 reflexions, ^3P); (*d*) $D_{\rm fi}$(**r**, 138 reflexions, ζ).

8.4. *Theoretical densities*

The static theoretical molecular density $\rho_{\rm th}^{\rm mol}(\mathbf{r})$ for C_2H_2 was obtained by the SCF–LCAO–MO method (Roothaan, 1951) with a computer program written by Van Duijnen & Thole (1977). A large GTO basis set (10,6,2/5,2) contracted to (6,4,2/4,2), including polarization functions for both C and H (Ruysink & Vos, 1974), was used for the calculation of the atomic and molecular wavefunctions. The bond lengths C≡C = 1·2033 and C–H = 1·0605 Å (Raman values; Fast & Welsh, 1972) were taken.

For the thermal smearing of the density, average values of the corresponding thermal parameters of refinements *A*3 and *C*5 (Table 5) were used with the program *BEDGOLV* (Ruysink & Vos, 1974). Because *BEDGOLV* cannot deal with non-linear motions, for the libration only the (coupled) librational parts $U_\perp(L,\mathrm{C})$ and $U_\perp(L,\mathrm{H})$ with $L = 0{\cdot}0187$ rad^2 were considered. The components $T_\parallel$ and $T_\perp$ for the translation of the molecule as a whole were obtained from the residual U values for C, thus

$$T_\parallel = U_\parallel(\mathrm{C}), \quad T_\perp = U_\perp(\mathrm{C}) - U_\perp(L,\mathrm{C}).$$

The residual values for H,

$$\Delta U_\parallel(\mathrm{H}) = U_\parallel(\mathrm{H}) - T_\parallel,$$
$$\Delta U_\perp(\mathrm{H}) = U_\perp(\mathrm{H}) - U_\perp(L,\mathrm{H}) - T_\perp,$$

were accounted for as uncoupled vibrations.

The static and dynamical theoretical deformation densities

$$D_{\rm th}(\mathbf{r}) = \rho_{\rm th}^{\rm mol}(\mathbf{r}) - \rho_{\rm th}^{\rm atom}(\mathbf{r}),$$

with corresponding atoms at the same positions in the two ρ maps, are shown in Fig. 7.

9. Discussion

9.1. *Positional and thermal parameters*

For refinement *C*5 (^3P refinement, Table 5) the C≡C distance is 1·178 (2) Å, including librational shorten-

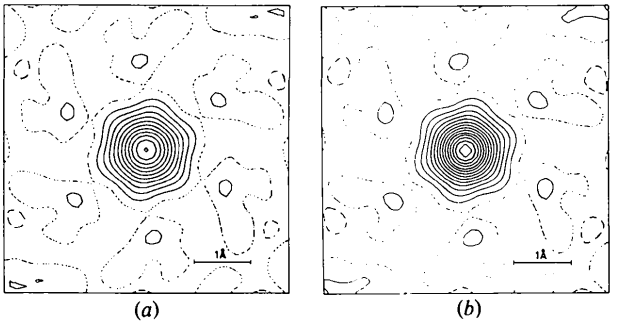

Fig. 6. Deformation density distributions in the plane perpendicular to C≡C and through the inversion centre. (*a*) D(**r**, 138 reflexions, ^3P); (*b*) D(**r**, 138 reflexions, ζ).

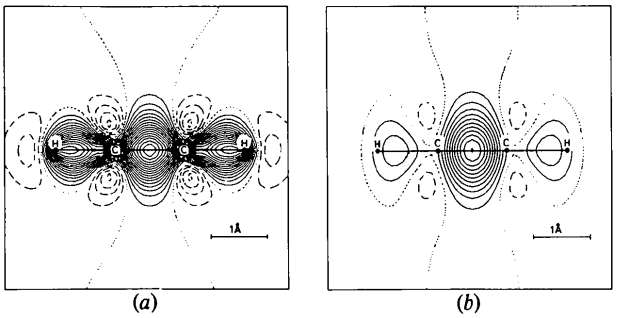

(*a*) (*b*)

Fig. 7. (*a*) Static and (*b*) dynamic theoretical deformation densities for C_2H_2 (for calculation see text).

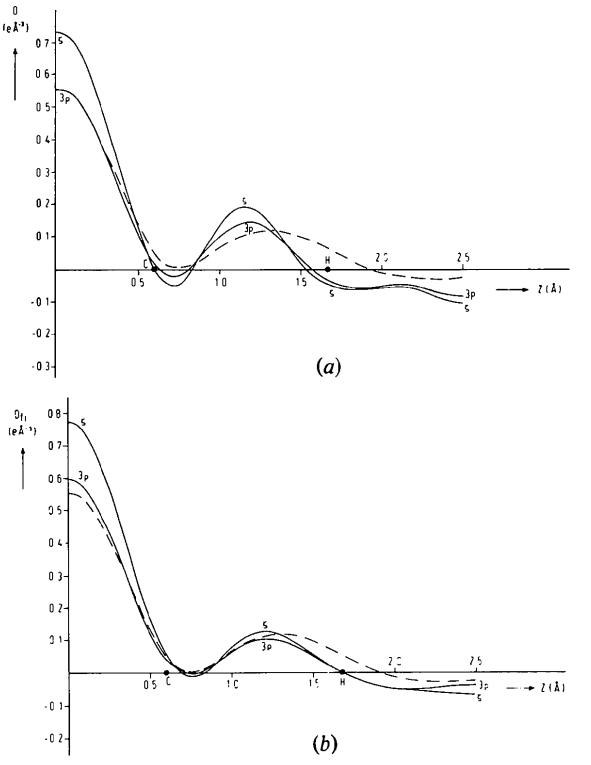

Fig. 8. (*a*) Deformation densities $D(Z)$ along the C≡C direction for 138 independent reflexions plus dynamic theoretical deformation density (see text). (*b*) Corresponding filtered densities plus dynamic theoretical deformation density. Solid lines: densities from refinements *C*5 (^3P scattering factors) and *A*3 (ζ scattering factors). Dashed lines: theoretical values.

ing. For refinement *A*3 (ζ refinement) this value is 1·183 (2) Å. Neither value is significantly different from the high-order ($\sin\theta/\lambda > 0{\cdot}55$ Å^{-1}) value of 1·182 (2) Å or from the neutron diffraction value of 1·180 (6) Å (Koski, 1975*a*). If the C≡C bond length of 1·2033 (2) Å found in the gas phase is taken to be correct for the solid, as was assumed during the refinements, we find from the librational shortening $\overline{(\varphi^2)}^{1/2}$ values of 8·2 and 7·4° for the refinements *C*5 and *A*3 respectively. The $\overline{u^2}$(C) value is 0·053 Å^2 for *C*5 and 0·051 Å^2 for *A*3. In particular the librational part of the thermal motion is high. This is in agreement with the low frequencies observed for the librational modes and with the reorientation of the molecules as discussed in § 2. These motions can hardly be expected to be harmonic, in contradistinction to the model adopted during the refinement.

9.2. *Discussion of the electron densities*

The bonding features along the C≡C direction are depicted in Fig. 8. The differences between the experimental curves in Fig. 8(*a*) and (*b*) correspond to the $D_f(Z)$ curve shown in Fig. 4 and discussed in § 8.1. Because of the omission of the monopole deformations, the $D_{fi}(Z)$ curves of Fig. 8(*b*) are not expected to represent the true bonding effect, especially at the atomic positions. As the monopole deformations have zero slope at the atomic positions (apart from contributions from neighbouring atoms), at C and H the slopes in the $D_{fi}(Z)$ curve are comparable with those in the theoretical curve. For the ^3P refinement especially, there is good agreement between theory and experiment. According to theoretical SCF calculations on molecules containing H atoms, at H the density is contracted, leading to a polarized H atom with scattering factor f(H,pol) (§ 6.3) (Stewart, Bentley & Goodman, 1975). Calculation of the dynamical theoretical difference map

$$D_{th}(\mathbf{r}) = \rho_{th}^{mol}(\mathbf{r}) - \rho_{th}^{atoms}(\mathbf{r}),$$

by subtracting contracted H atoms with f(H,pol), rather than SCF diffuse H atoms, from $\rho_{th}^{mol}(\mathbf{r})$, would have dropped $D_{th}(\mathbf{r})$ by 0·05 e Å^{-3} to 0·01 e Å^{-3} at the position of H, giving good agreement with the experimental curves of Fig. 8(*b*). This shows that for H, as expected, the monopole deformation is described well by replacing the diffuse SCF atom by the polarized atom. For C the good agreement indicates that evidently the monopole deformation is very small. Also Figs. 5(*c*), (*d*) and 7(*b*) show that there is a strong resemblance between the experimental filtered and the dynamical theoretical deformation maps for C≡C. Characteristic features are, for instance, the quadrupolar-type deformation around C and the slightly positive density observed at large distances from the centre in the direction perpendicular to C≡C. For the theoretical map the positive density at C≡C extends slightly further than for the $D_{fi}(\mathbf{r})$ maps. It must therefore be concluded that the present experimental evidence has given no indication of errors in the theoretical density.

9.3. *Reliability of the experimental results*

As has been discussed in the previous sections, strong correlation exists between the different param-

eters (Table 6). This is mainly due to the fact that, because of the small cell and the strong thermal motion, the reflexion set was restricted to $0{\cdot}14 < \sin\theta/\lambda < 0{\cdot}80$ Å^{-1}. This correlation hampers both a detailed discussion of the density distribution (§ 9.2) and the determination of molecular properties such as quadrupole moments (Stewart, 1972). This is clearly shown by the calculation of the quadrupole moment Θ from the parameters of refinements $A3$ and $A4$; these refinements only differ in that in $A4$ the C atom has been fixed at 0·003 Å from the $A3$ position. For $A3$, $\Theta = 3{\cdot}3$ and for $A4$ $\Theta = 2{\cdot}6 \times 10^{-39}$ Cm^2; the experimental value for a free C_2H_2 molecule is $1{\cdot}0 \times 10^{-39}$ Cm^2 (Gordy, Smith & Trambarulo, 1953). The large difference between $\Theta(A3)$ and $\Theta(A4)$ is mainly due to the change in H dipole, induced by the change in the position of H (which is constrained to C). This clearly shows that for this type of work compounds containing H atoms are not very suitable unless the H (and heavy-atom) positions are accurately known from a neutron diffraction study.

Correlation between scale, temperature factors, monopole populations and type of scattering factors can be avoided to a large extent by direct experimental determination of the scale K and deduction of the **U** tensors from neutron diffraction data. Only in that case, more detailed information on the radial functions $\rho_p(l,r_p)$ (formula 6) may be obtained. Accurate determination of K is hard to achieve for mosaic crystals (Stevens & Coppens, 1975), however. Transference of the 'neutron U_{ij} values' to X-ray data requires (apart from the assumption that the convolution approximation is valid), accurate corrections for TDS (Kroon & Vos, 1979) and crystals of comparable quality for the two experiments.

In conclusion, it may be mentioned that the present compound has presented an unfavourable case for an accurate analysis of the electron density distribution. However, the simplicity of the compound and the high symmetry of the crystals have made it feasible to compare the results for different types of refinement, and the study has shown which difficulties may be encountered in this type of work.

The authors are deeply indebted to professor Dr Aafje Vos for her interest, guidance and stimulating discussions. We wish to thank Dr J. L. de Boer and Dr P. Th. van Duijnen for critical reading of the manuscript, Drs H. R. van der Wal for the improvements in the program *VALRAY* and Dr P. Th. van Duijnen and Drs R. J. van der Wal for the quantum-mechanical calculations. Part of the investigations was supported by the Foundation for Fundamental Research of Matter with X-rays and Electron Rays (FOMRE) with financial aid from the Netherlands Organization for the Advancement of Pure Research (ZWO). The computations were carried out on the CYBER 74-18 computer of the University of Groningen.

References

ALBERT, S. & RIPMEESTER, J. A. (1972). *J. Chem. Phys.* **57**, 3953–3959.

ANDERSON, A. & SMITH, W. H. (1966). *J. Chem. Phys.* **44**, 4216–4219.

BECKER, P. J. & COPPENS, P. (1974). *Acta Cryst.* A**30**, 129–153.

BENTLEY, J. & STEWART, R. F. (1976). *Acta Cryst.* A**32**, 910–914.

BOTTGER, G. L. & EGGERS, D. F. JR (1964). *J. Chem. Phys.* **40**, 2010–2017.

BOTTGER, G. L. & EGGERS, D. F. JR (1966). *J. Chem. Phys.* **44**, 4366.

CLEMENTI, E. (1965). *Tables of Atomic Functions*. San José Research Laboratory, International Business Machines Corporation, San José, California.

CLEMENTI, E. & POPKIE, H. (1972). *J. Chem. Phys.* **57**, 4870–4883.

COPPENS, P. (1975). *MTP International Review of Science: Physical Chemistry, Series* 2, Vol. 11, pp. 21–56, edited by J. M. ROBERTSON. London: Butterworths.

CROMER, D. T. & MANN, J. B. (1968). *Acta Cryst.* A**24**, 321–324.

DAWSON, B. (1967). *Proc. R. Soc. London Ser. A*, **298**, 255–263.

FAST, H. & WELSH, H. L. (1972). *J. Mol. Spectrosc.* **41**, 203–221.

GORDY, W., SMITH, W. V. & TRAMBARULO, R. F. (1953). *Microwave Spectroscopy*. New York: John Wiley.

HEHRE, W. J., STEWART, R. F. & POPLE, J. A. (1969). *J. Chem. Phys.* **51**, 2657–2664.

HELLNER, E. (1977). *Acta Cryst.* B**33**, 3813–3816.

HELMHOLDT, R. B. & VOS, A. (1977). *Acta Cryst.* A**33**, 456–465.

HIRSHFELD, F. L. (1971). *Acta Cryst.* B**27**, 769–781.

ITO, M., YOKOYAMA, T. & SUZUKI, M. (1970). *Spectrochim. Acta Part A*, **26**, 695–705.

JOHNSON, C. K. (1969). *Acta Cryst.* A**25**, 187–194.

JOHNSON, C. K. (1970). *ORTEP* II. Report ORNL-3794, 2nd revision. Oak Ridge National Laboratory, Tennessee.

KOSKI, H. K. (1975*a*). *Acta Cryst.* B**31**, 933–935.

KOSKI, H. K. (1975*b*). *Cryst. Struct. Commun.* **4**, 337–341.

KOSKI, H. K. (1975*c*). *Cryst. Struct. Commun.* **4**, 343–347.

KOSKI, H. K. (1975*d*). *Z. Naturforsch. Teil A*, **30**, 1028–1031.

KOSKI, H. K. & SÁNDOR, E. (1975). *Acta Cryst.* B**31**, 350–353.

KRIKORIAN, E. (1957). PhD Thesis, Columbia Univ.

KROON, P. A. & VOS, A. (1979). *Acta Cryst.* A**35**, 675–684.

MEISINGSETH, E. & CYVIN, S. J. (1961). *Acta Chem. Scand.* **15**, 2021–2025.

MOOY, H. H. (1932). *Commun. Kamerlingh Onnes Lab. Univ. Leiden*, **223**, 1–8.

NES, G. J. H. VAN & VAN BOLHUIS, F. (1975). *Acta Cryst.* A**31**, S227.

NES, G. J. H. VAN & VAN BOLHUIS, F. (1978). *J. Appl. Cryst.* **11**, 206–207.

NES, G. J. H. VAN & VOS, A. (1978). *Acta Cryst.* B**34**, 1947–1956.
PAULING, L. (1960). *The Nature of the Chemical Bond*, 3rd ed. Ithaca: Cornell Univ. Press.
PERLMAN, I., GILBOA, H. & RON, A. (1972). *J. Magn. Reson.* **7**, 379–387.
PERLMAN, I., GILBOA, H. & RON, A. (1973). *J. Magn. Reson.* **9**, 467–473.
PRICE, R. F. & MASLEN, E. N. (1978). *Acta Cryst.* A**34**, 173–183.
ROOTHAAN, C. C. J. (1951). *Rev. Mod. Phys.* **23**, 69–89.
RUYSINK, A. F. J. & VOS, A. (1974). *Acta Cryst.* A**30**, 497–502.
SCHEIE, C. E., PETERSON, E. M. & O'REILLY, D. E. (1973). *J. Chem. Phys.* **59**, 2758–2759.
SCHWARTZ, Y. A., RON, A. & KIMEL, S. (1969). *J. Chem. Phys.* **51**, 1666–1667.
SCHWARTZ, Y. A., RON, A. & KIMEL, S. (1971). *J. Chem. Phys.* **54**, 99–105.
SMITH, W. H. (1969). *Chem. Phys. Lett.* **3**, 464–466.
STEVENS, E. D. & COPPENS, P. (1975). *Acta Cryst.* A**31**, 612–619.
STEWART, R. F. (1972). *J. Chem. Phys.* **57**, 1664–1668.
STEWART, R. F. (1974). *VALRAY* 1974 system. Department of Chemistry, Carnegie-Mellon Univ., Pittsburgh, Pennsylvania 15213, USA.
STEWART, R. F. (1976). *Acta Cryst.* A**32**, 565–574.
STEWART, R. F. (1977). *Isr. J. Chem.* **16**, 124–131.
STEWART, R. F., BENTLEY, J. & GOODMAN, B. (1975). *J. Chem. Phys.* **63**, 3786–3793.
STEWART, R. F., DAVIDSON, E. R. & SIMPSON, W. T. (1965). *J. Chem. Phys.* **42**, 3175–3187.
SUGAWARA, T. & KANDA, E. (1952). *Sci. Rep. Res. Inst. Tôhoku Univ. Ser. A*, **4**, 607–614.
TABATA, Y., SAITO, B., SHIBANO, H., SOBUE, H. & OSHIMA, K. (1964). *Makromol. Chem.* **76**, 89–98.
TIMMERMANS, J. (1961). *J. Phys. Chem. Solids*, **18**, 1–8.
VAN DUIJNEN, P. TH. & THOLE, B. T. (1977). Chemistry Department, Univ. of Groningen, The Netherlands.
WAHL, W. (1913). *Proc. R. Soc. London Ser. A*, **89**, 327–339.
WAL, H. R. VAN DER (1978). Update of *VALRAY* 1974 program. Private communication.
WASHER, F. E. (1935). *Proc. Indian Acad. Sci.* **45**, 222–228.
WILLIS, B. T. M. & PRYOR, A. W. (1975). *Thermal Vibrations in Crystallography*, 1st ed., p. 202. Cambridge Univ. Press.
WILSON, E. B. JR (1941). *J. Chem. Phys.* **9**, 76–84.
ZACHARIASEN, W. H. (1967). *Acta Cryst.* **23**, 558–564.
ZACHARIASEN, W. H. (1968). *Acta Cryst.* A**24**, 212–216.

Acta Cryst. (1979). B**35**, 2593–2601

Single-Crystal Structures and Electron Density Distributions of Ethane, Ethylene and Acetylene.

III.* Single-Crystal X-ray Structure Determination of Ethylene at 85 K

BY GERARD J. H. VAN NES AND AAFJE VOS

Laboratorium voor Structuurchemie, Rijksuniversiteit Groningen, Nijenborgh 16, 9747 *AG, Groningen, The Netherlands*

(*Received* 27 *November* 1978; *accepted* 11 *June* 1979)

Abstract

Crystalline C_2H_4 at 85 K is monoclinic, $a = 4{\cdot}626$ (1), $b = 6{\cdot}620$ (2), $c = 4{\cdot}067$ (2) Å, $\beta = 94{\cdot}39$ (2)°, space group $P2_1/n$, $Z = 2$. The intensities of all reflexions with $\sin\theta/\lambda < 1{\cdot}07$ Å^{-1} were measured at two ψ values on a Nonius four-circle diffractometer. A valence analysis with multipole deformation terms up to octopole on C and up to quadrupole on H has been performed by anisotropic least-squares refinement on I, including extinction, on the 1295 independent reflexion intensities. Both ζ and SCF scattering factors were considered. The position of H was constrained to that of C. $R_w(I;\zeta) = 0{\cdot}0231$ and $R_w(I;^3P) = 0{\cdot}0243$ for 38 and 35 independent variables respectively; $\overline{u^2}$(C) = 0·036 Å^2, $(\overline{\varphi^2})^{1/2} = 8°$ for the axis perpendicular to C=C and in the molecular plane. The dipole at H is found to lie along the C–H bond. Although less pronounced, correlation effects as discussed for C_2H_2 [van Nes & van Bolhuis (1979). *Acta Cryst.* B**35**, 2580–2593] still occur. All Fourier maps are based on the reflexions with $I > 0$. Inclusion of monopole terms in the filtered deformation density map is prevented by the correlation between the radial parameters (including the scale). Apart from the omitted monopole deformations the agreement between theory and experiment is satisfactory.

* Part II: van Nes & van Bolhuis (1979).

0567-7408/79/112593-09$01.00